Outer Shape of Molecules as Probed by Ground-State Atoms from H to Ar

Shigeo Hoshino and Koichi Ohno*

Contribution from the Department of Chemistry, Graduate School of Science, Tohoku University, Aramaki, Aoba-ku, Sendai 980-77, Japan

Received September 26, 1996. Revised Manuscript Received June 5, 1997[⊗]

Abstract: In order to clarify systematic trends of governing outer shape of molecules, isopotential energy contours of hydrogen and nitrogen molecules as probed by ground-state atoms from H to Ar have been studied. Periodicity and some interesting patterns have been found for the outer profiles of molecules. When the exchange repulsion energy is dominant, repulsive walls of potential energy curves show a simple exponential decay with hardness depending on the ionization potentials. When anisotropic interactions reduce the exchange repulsion energy effectively, outer shape of molecules probed by atoms are deformed into various forms, even for simple diatomic molecules such as hydrogen and nitrogen.

1. Introduction

The outer boundary shape of molecules is an important concept which is widely used in many fields of scientific investigations. The concept of van der Waals (VDW) radii of atoms arose from careful analysis of crystal packing data.[1−3] In the Kihara model,[4] which has been used for statistical thermodynamic calculations of molecular systems, the shape of a molecule is associated with a suitable undeformable hard convex core, for instance a regular tetrahedron for CF_4 and a thin hexagonal plate for C_6H_6. Outer shapes of molecules are also extremely important in understanding chromatographic retention in analytical chemistry[5] and also in biophysical properties.[6] The solvent accessible area was defined by Lee and Richards[7] as the surface pushed outward from the VDW surface by a distance equal to the radius of a rolling probe sphere, and the VDW surface was more precisely defined as the contact surface (part of the VDW surface accessible to a probe sphere).[8] The VDW surface was further used as the boundary surface which separates exterior electron densities from the interior densities in relation to relative activities of molecular orbitals in chemi-ionization reactions known as Penning ionization.[9] There remain, however, the following serious problems with the VDW radii and VDW surface. (1) Anisotropy of the VDW radii should be considered when the chemical structure is highly anisotropic.[10−12] (2) VDW radii should depend on the kinds of atoms interacting each other. (3) The VDW surface as the boundary to the probing species should vary with the relative velocities of collisions in scattering experiments or with applied external forces such as those exerted in AFM experiments.[13]

The spherical VDW model has been corrected for anisotropic effects; nitrogen and oxygen lone pairs were assigned to substituents with their own parameters,[10] and the distance to a hydrogen atom in a head on approach was defined with an offset of the potential center 7.7% into the C−H bond.[11] Recently, in the study of geometrical structures for complexes of some molecules with Cl_2 and HCl,[12a] which were determined by microwave spectroscopy,[14] it has been suggested that the VDW radius of the Cl atom in Cl_2 is smaller along the Cl_2 internuclear axis than perpendicular to it. This propensity has been confirmed theoretically with the aid of *ab initio* calculations for the Cl_2 + He and HCl + He systems.[12b]

Another approach for representing outer shape of molecules is to utilize the sum of pairwise additive potentials. An application of this type has been made for copper phthalocyanine by using Lennard-Jones atomistic potentials.[15] Although such empirical model potentials as the Lennard-Jones function and the Morse function have been successfully applied to the analyses of experimental data for small clusters[16,17] as well as AFM[18] and also applied to molecular mechanics calculations,[19,20] the nature of interactions is not so simple as the functions might imply. One of important factors to be considered is the anisotropy of real potentials, which in general cannot be expressed by the model functions in a pairwise form. Another factor completely missing in the model functions is the effect

[⊗] Abstract published in *Advance ACS Abstracts,* August 1, 1997.

(1) Pauling, L. *The Nature of The Chemical Bond*, 3rd ed.; Cornell University: Ithaca, NY, 1960.
(2) Bondi, A. *J. Phys. Chem.* **1964**, *68*, 441−451.
(3) Chauvin, R. *J. Phys. Chem.* **1992**, *96*, 9194−9197.
(4) (a) Kihara, T. *Rev. Mod. Phys.* **1953**, *25*, 831−843. (b) Kihara, T. *Rev. Mod. Phys.* **1955**, *27*, 412−423.
(5) Rohrbaugh, R. H.; Jurs, P. C. *Anal. Chem.* **1987**, *59*, 1048−1054.
(6) Dubois, J. E.; Doucet, J. P.; Yue, S. Y. In *Molecules in Physics, Chemistry, and Biology*; Maruani, J., Ed.; Kluwer Academic: Dordrecht, 1988; Vol. 1, pp 173−204.
(7) Lee, B.; Richards, F. M. *J. Mol. Biol.* **1971**, *55*, 379−400.
(8) Richards, F. M. *Annu. Rev. Biophys. Bioeng.* **1977**, *6*, 151−176.
(9) Ohno, K.; Mutoh, H.; Harada, Y. *J. Am. Chem. Soc.* **1983**, *105*, 4555−4561.
(10) (a) Allinger, N. L.; Chung, D. Y. *J. Am. Chem. Soc.* **1976**, *98*, 6798−6803. (b) Profeta, S., Jr.; Allinger, N. L. *J. Am. Chem. Soc.* **1985**, *107*, 1907−1918. (c) Allinger, N. L.; Rahman, M.; Lii, J.-H. *J. Am. Chem. Soc.* **1990**, *112*, 8293−8307. (d) Schmitz, L. R.; Allinger, N. L. *J. Am. Chem. Soc.* **1990**, *112*, 8307−8315.
(11) (a) Allinger, N. L. *J. Am. Chem. Soc.* **1977**, *99*, 8127−8134. (b) Lii, J.-H.; Allinger, N. L. *J. Am. Chem. Soc.* **1989**, *111*, 8576−8582.
(12) (a) Legon, A. C. *Chem. Phys. Lett.* **1995**, *237*, 291−298. (b) Peebles, S. A.; Fowler, P. W.; Legon, A. C. *Chem. Phys. Lett.* **1995**, *240*, 130−134.
(13) Binnig, G.; Quate, C. F.; Gerber, Ch. *Phys. Rev. Lett.* **1986**, *56*, 930−933.
(14) See, for example: (a) Legon, A. C.; Lister, D. G.; Thorn, J. C. *J. Chem. Soc., Faraday Trans.* **1994**, *90*, 3205−3212. (b) Fraser, G. T.; Pine, A. S. *J. Chem. Phys.* **1989**, *91*, 637−645.
(15) Liu, D.-J.; Selinger, R. L. B.; Weeks, J. D. *J. Chem. Phys.* **1996**, *105*, 4751−4760.
(16) Jena, P.; Rao, B. K.; Khanna, S. N. *Physics and Chemistry of Small Clusters*; Plenum: New York, 1987.
(17) Scoles, G. *The Chemical Physics of Atomic and Molecular Clusters*; North-Holland: Amsterdam, 1990.
(18) Sasaki, N.; Tsukada, M. *Jpn. J. Appl. Phys.* **1995**, *34*, 3319−3324.
(19) Boyd, D. B.; Lipkowitz, K. B. *J. Chem. Educ.* **1982**, *59*, 269−274.
(20) Cox, P. J. *J. Chem. Educ.* **1982**, *59*, 275−277.

S0002-7863(96)03376-8 CCC: $14.00

Table 1. Electronic States of Interacting Systems To Be Studied

probe atom	electronic state symmetry $C_{\infty v}$	C_s	C_{2v}
H(^{2}S), Li(^{2}S), F(^{2}P), Na(^{2}S), Cl(^{2}P)	$^2\Sigma^+$	^{2}A′	^{2}A$_1$
He(^{1}S), Be(^{1}S), Ne(^{1}S), Mg(^{1}S), Ar(^{1}S)	$^1\Sigma^+$	^{1}A′	^{1}A$_1$
B(^{2}P), Al(^{2}P)	$^2\Pi$	^{2}A′	^{2}B$_2$
C(^{3}P), Si(^{3}P)	$^3\Sigma^-$	^{3}A″	^{3}A$_2$
N(^{4}S), P(^{4}S)	$^4\Sigma^-$	^{4}A″	^{4}A$_2$
O(^{3}P), S(^{3}P)	$^3\Pi$	^{3}A″	^{3}B$_1$

of potential crossing, which possibly yields unusual up and down structures in potential energy curves.

In the present study, isopotential energy contours of simple diatomic molecules, $H_2(^1\Sigma_g^+)$ and $N_2(^1\Sigma_g^+)$, are studied by *ab initio* calculations using ground-state atoms from H to Ar as a probe characterizing outer profiles of molecules. Systematic trends reflecting periodicity and some interesting patterns, which cannot be adequately modeled by current conventional approaches using pair-potentials, are found for outer shape of molecules. The natures of outer profiles of molecules are discussed in terms of interorbital interactions and periodicity in electronic configurations.

2. Calculations

Potential energy curves for various directions θ from the molecular axis were obtained as functions of the distance R between a probe atom and the center of symmetry of a molecule. Nuclear positions of molecules were fixed at ground-state experimental geometries. The potential energy along a certain direction $V(R)$ is obtained from the following equation

$$V(R) = E_{MA} - E_M - E_A \quad (1)$$

where E_M, E_A, and E_{MA} are the total energy of the isolated molecule (M), the isolated atom (A), and the interacting system (MA), respectively. For full counterpoise corrections[21] and electron correlation effects, Gaussian 86[22a] and 92[22b] programs were employed. The effects of electron correlation on the potential energy were carefully investigated for $N_2(^1\Sigma_g^+)$ + C(^{3}P) at the MP2, MP4(SDTQ), CCSD, QCISD, and QCISD(T) levels. For a systematic comparison, potential energy calculations were performed at the MP2 level. In order to obtain contour maps of the closest position of a probe atom for given potential energies, a number of single point *ab initio* calculations were performed. Isopotential energy contours were drawn with the aid of a spline program on a personal computer. Isopotential energy contours or outer shapes of molecules so obtained were fitted to an analytic functional form using a fitting program.[23]

Interacting systems have a $C_{\infty v}$ symmetry for the collinear approach of probe atoms ($\theta = 0°$), C_{2v} for the vertical ($\theta = 90°$), and C_s for the others. Electronic states of the interacting systems investigated are listed in Table 1.

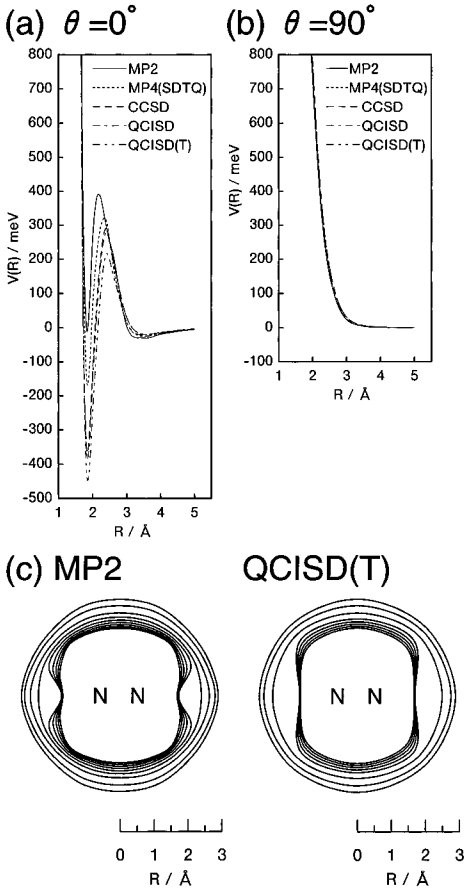

Figure 1. Potential energy curves of $\theta = 0°$ (a) and 90° (b) for $N_2(^1\Sigma_g^+)$ + C(^{3}P) calculated by some correlation methods; MP2 (—), MP4(SDTQ) (- - -), CCSD (— — —), QCISD (— - —), and QCISD(T) (— - - —). The distance R is measured from the center of symmetry of the molecule. (c) Isopotential energy contours obtained from MP2 and QCISD(T) calculations. Outermost lines are the contours of 50 meV and the nth lines ($n \geq 2$) from the outside correspond to the contours of $(n - 1) \times 100$ meV.

An efficient basis set for calculations of interaction energies have been studied.[24] On this basis, augmentation of the standard diffuse[25] and polarization[25] functions was made to split-valence type basis sets (5-21G for Li and Be, 4-31G for H, He, and the other first row atoms, 6-21G for Na and Mg, and 6-31G for the other second row atoms). Polarization d functions for the first and second row atoms are of a six component type. The 5-21G basis set without diffuse and polarization functions has been found to be adequate for Li.[26]

For more detailed analysis, the difference of electron densities $\Delta\rho$ between interacting and isolated systems was also investigated; the following quantities were calculated

$$\Delta\rho = \rho_{MA} - \rho_M - \rho_A \quad (2)$$

where ρ_M, ρ_A, and ρ_{MA} are the total electron density at a certain geometrical point for M, A, and MA, respectively.

3. Results

3.1. Effects of Electron Correlation on Potential Energy. In Figure 1, potential energy curves of $\theta = 0°$ (a) and 90° (b)

(21) Boys, S. F.; Bernardi, F. *Mol. Phys.* **1970**, *19*, 553−566.

(22) (a) Frisch, M. J.; Binkley, J. S.; Schlegel, H. B.; Raghavachari, K.; Melius, C. F.; Martin, R. L.; Stewart, J. J. P.; Bobrowicz, F. W.; Rohlfing, C. M.; Kahn, L. R.; DeFrees, D. J.; Seeger, R.; Whiteside, R. A.; Fox, D. J.; Fluder, E. M.; Pople, J. A. Gaussian 86; Gaussian, Inc.: Pittsburgh, PA, 1987. Revised for a HITAC M-880 by Hirano, T.; Nomura, O.; Murao, H. (b) Frisch, M. J.; Trucks, G. W.; Head-Gordon, M.; Gill, P. M.; Wong, M. W.; Foresman, J. B.; Johnson, B. G.; Schlegel, H. B.; Robb, M. A.; Replogle, E. S.; Gomperts, R.; Andres, J. L.; Raghavachari, K.; Binkley, J. S.; Gonzalez, C.; Martin, R. L.; Fox, D. J.; DeFrees, D. J.; Baker, J.; Stewart, J. J. P.; Pople, J. A. Gaussian 92; Gaussian, Inc.: Pittsburgh, PA, 1992.

(23) Nakagawa, T.; Oyanagi, Y. In *Recent Developments in Statistical Inference and Data Analysis*; Matusita, K., Ed.; North-Holland: Amsterdam, 1980; pp 221−225.

(24) Chałasiński, G.; Gutowski, M. *Chem. Rev.* **1988**, *88*, 943−962 and references cited therein.

(25) Hehre, W. J.; Radom, L.; Schleyer, P. v. R.; Pople, J. A. *Ab Initio Molecular Orbital Theory*; John Wiley & Sons: New York, 1986.

(26) Ohno, K.; Sunada, S. *Proc. Indian Acad. Sci. (Chem. Sci.)* **1994**, *106*, 327−337.

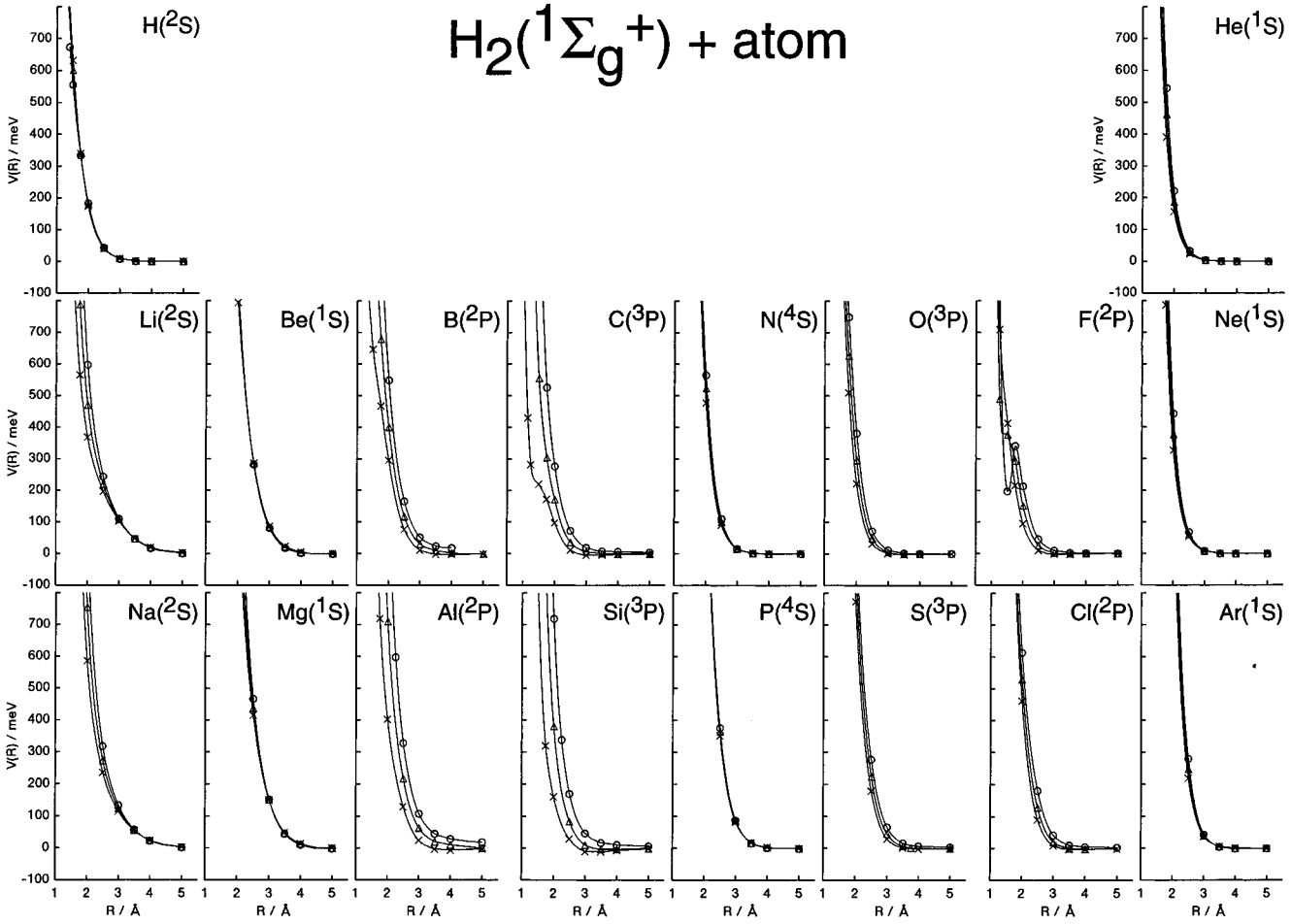

Figure 2. Potential energy curves of $H_2(^1\Sigma_g^+)$ in interaction with a probe atom from $H(^2S)$ to $Ar(^1S)$. The distance R is measured from the center of symmetry of the molecule. The angles θ from the collinear direction are $\theta = 0°$ (○), 45° (△), and 90° (×), respectively.

for $N_2(^1\Sigma_g^+)$ + $C(^3P)$ calculated by some correlation methods are shown, respectively. Although well depths for the short-range minima are considerably different for $\theta = 0°$, respulsive parts of all potential curves are almost overlapping, especially for $\theta = 90°$.

Isopotential energy contours based on MP2 and QCISD(T) level calculations are shown in Figure 1(c). The short-range wells were omitted, since the inner wells are not important to know the outer shape of a molecule. In Figure 1(c), outer profiles of nitrogen molecule probed by C atom are qualitatively similar between MP2 and QCISD(T), although interactions in this system are markedly anisotropic among 36 cases. Thus, systematic comparison of outer profiles of molecules were made at the MP2 level in the present study.

3.2. *Ab Initio* Potential Energy Curves. Calculated *ab initio* potential energies $V(R)$ for fixed angles of $\theta = 0°$, 45°, and 90° are shown for $H_2(^1\Sigma_g^+)$ in Figure 2 and for $N_2(^1\Sigma_g^+)$ in Figure 3, respectively. Potential energy curves for other angles such as $\theta = 22.5°$ and 67.5° were not shown for the simplicity, since they are almost simply intermediate between those for $\theta = 0°$ and 45° and between those for $\theta = 45°$ and 90°, respectively. The following features are commonly found in Figures 2 and 3.

(1) Potential energy curves are almost decreasing functions of the distance R.

(2) Relative positions of potential energy curves for $\theta = 0°$, 45°, and 90° vary depending on the kinds of probe atoms.

(3) Potential energy curves for the second row atoms are more or less similar to those for the corresponding first row atoms.

3.3. *Ab Initio* Isopotential Energy Contours. In Figures 4 and 5, contour curves of the nearest location of a probe atom are drawn for $H_2(^1\Sigma_g^+)$ and for $N_2(^1\Sigma_g^+)$, respectively. The nth lines from the outside correspond to the contours of $n \times 100$ meV. Each contour curve represents an outer profile of the rigid molecule probed by an atom with a certain kinetic energy.

Although hydrogen and nitrogen are simple diatomic molecules, varieties of profiles are found. The profiles exhibit (1) a periodicity related to the electronic configuration and (2) several prototypes arising from peculiar interactions depending on the directions as well as on the kinds of atomic probes. In relation to the periodicity, the profiles become larger on going from the first row to the corresponding second row probe atoms. This can be ascribed to the difference in the atomic size.

3.4. Functional Form of Repulsive Interaction and Analytical Fitting for Potential Energy Surfaces. Since contour curves deform into various forms as can be seen in Figures 4 and 5, it is important to choose the suitable functional form for the repulsive interaction. There are two types of typical functional forms for the short-range repulsive interaction; one is proportional to the inverse power of distance, $A(1/R^n)$, and the other is a simple exponential function, $A \exp(-aR)$. Parameters n and a are a measure of the hardness in the repulsive potential, which can be evaluated from linear dependences of ln $V(R)$ on the distance ln R and R for $V(R) > 0$, respectively.

In Table 2, parameter values a obtained for the energy range between 100 and 800 meV are listed with the square-root of the lowest atomic ionization potentials (IP/eV). It is found that there are the following orders in the magnitude of the steepness parameters for $\theta = 0°$ and 90°.

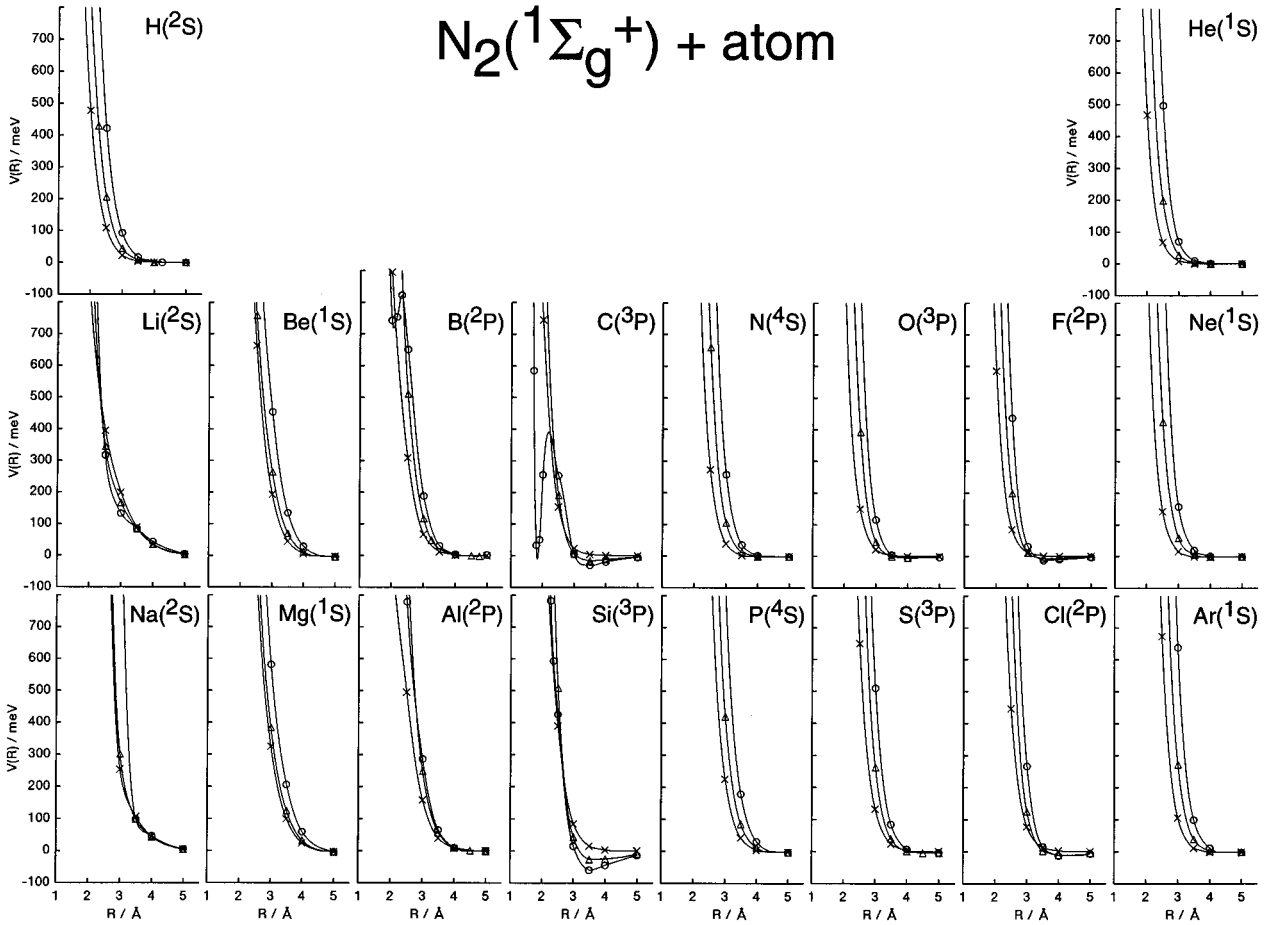

Figure 3. Potential energy curves of $N_2(^1\Sigma_g^+)$ in interaction with a probe atom from H(^{2}S) to Ar(^{1}S). The distance R is measured from the center of symmetry of the molecule. The angles θ from the collinear direction are $\theta = 0°$ (○), 45° (△), and 90° (×), respectively.

alkali metal ($\sqrt{IP}$: 2.26−2.32) ≤ alkaline earth metal ($\sqrt{IP}$: 2.76−3.05) ≤H ($\sqrt{IP}$: 3.69) and Group 15 ($\sqrt{IP}$: 3.24−3.81) < rare gas ($\sqrt{IP}$: 3.97−4.96)

Since electron exchange repulsion depends on the extent of overlapping between the wave functions, these orders can be ascribed to radial asymptotic decay of the wave functions, which are simply related to the square-root of the lowest *IP*.[27,28] Electron distributions for rare gas atoms (high *IP* atoms) are more compact than those for alkali and alkaline earth metal atoms (low *IP* atoms), and the square-root of atomic *IP* values vary in good accordance with the above order of the steepness parameters, as shown in the parentheses. The same order for $H_2(^1\Sigma_g^+)$ and $N_2(^1\Sigma_g^+)$ is partly because their molecular *IP* values are nearly the same and also partly because *IP* values for probing atoms vary to a large extent from 5 to 25 eV.

On the other hand, the parameters n depend on the kind of molecules to lead larger values for $N_2(^1\Sigma_g^+)$ (3.91−11.94) than those for $H_2(^1\Sigma_g^+)$ (3.18−8.40) and also on the directions to yield larger differences between $\theta = 0°$ and 90° (0.01−3.14) than those for parameters a (0.01−0.67). Since a typical functional form of attractive term is $1/R^6$, repulsive parameter values of smaller than 6, such as 3.18 for $H_2(^1\Sigma_g^+)$ + Li(^{2}S), are not appropriate. Therefore, the Lennard-Jones type repulsive term of $1/R^n$ is not suitable for describing outer profiles of molecules.

Based on these findings, we propose the following function including Legendre polynomials $P_i(\cos\theta)$ for global potential energy surfaces $V(R, \theta)$.

$$V(R,\theta) = \sum_{i=0,2,4,6,8} P_i(\cos\theta)V_i(R) \quad (3)$$

$$V_i(R) = A_i \exp(-a_i R) + B_i \exp(-b_i R^2)\cos(c_i \pi R) \quad (4)$$

Here, A_i, a_i, B_i, b_i, and c_i are parameters to be determined. Potential energy functions for fixed angles $V_i(R)$ consist of two terms to represent unusual structures in potential energy curves; the first is pure repulsive part and the second is decreasing with oscillation. Parameter values obtained from analytic functional fitting and root mean square (rms) errors for contour curves (ΔR_{rms}) are listed for $H_2(^1\Sigma_g^+)$ in Table 3(a) and for $N_2(^1\Sigma_g^+)$ in Table 3(b), respectively. Since the boundary shapes or contours at certain potential energies are noted in the present study, the standard errors in the calculated shapes are shown as ΔR_{rms} in the unit of distance. Vanishing contributions of higher order terms are not retained in the table, although the Legendre expansion has been taken into account to the eighth order.

As can be seen in Figure 6 (parts a and b), contour curves give good agreement between *ab initio* calculation (a) and functional fitting (b). Although in eq 3 expanded terms were taken into account to the eighth orders, contributions of the sixth and eighth order terms were found to be negligibly small. In some cases, higher order terms were set equal to zero in the

(27) (a) Ahlrichs, R. *Chem. Phys. Lett.* **1973**, *18*, 521−524. (b) Hoffmann-Ostenhof, M.; Hoffmann-Ostenhof, T. *Phys. Rev. A* **1977**, *16*, 1782−1785. (c) Hoffmann-Ostenhof, T.; Hoffmann-Ostenhof, M.; Ahlrichs, R. *Phys. Rev. A* **1978**, *18*, 328−334.

(28) Katriel, J.; Davidson, E. R. *Proc. Natl. Acad. Sci. U.S.A.* **1980**, *77*, 4403−4406.

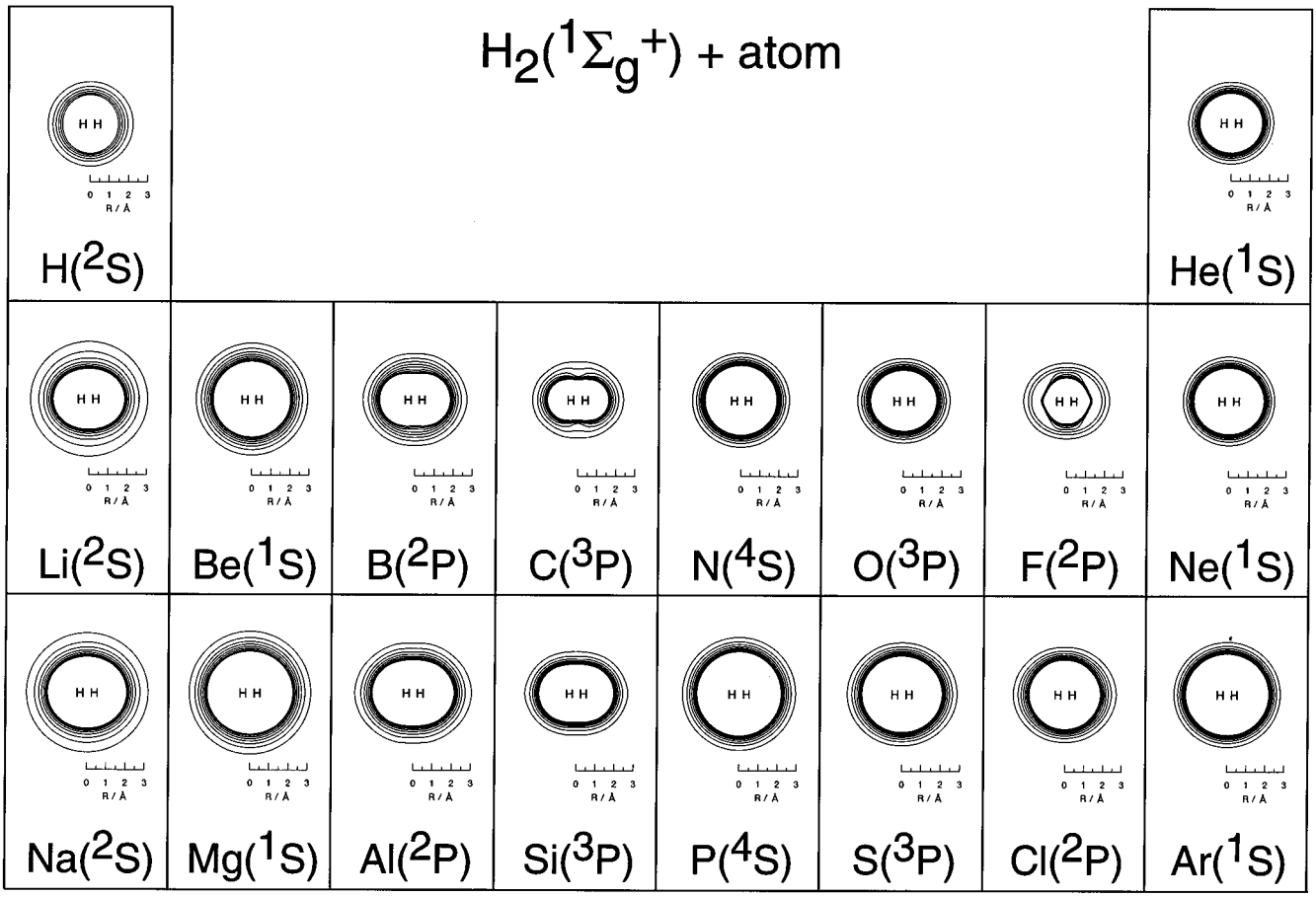

Figure 4. *Ab initio* isopotential energy contours of $H_2(^1\Sigma_g^+)$ in interaction with a probe atom from H(^{2}S) to Ar(^{1}S). The *n*th lines from the outside correspond to the contours of $n \times 100$ meV.

Table 2. Parameter Values (a/Å^{-1}) Fitted by the Repulsive Functional Form $V(R) = A \exp(-aR)$ and the Square-Root of the Lowest Atomic Ionization Potentials (*IP*/eV)

	$H_2(^1\Sigma_g^+)$		$N_2(^1\Sigma_g^+)$		
	$\theta = 0°$	$\theta = 90°$	$\theta = 0°$	$\theta = 90°$	$\sqrt{IP}$
H	2.34	2.60	2.95	2.89	3.69
He	3.58	3.60	3.83	3.80	4.96
Li	1.74	1.43	*a*	1.47	2.32
Be	2.34	2.19	2.26	2.51	3.05
B	2.40	*a*	*a*	2.49	2.88
C	2.68	*a*	*a*	3.18	3.36
N	3.18	3.25	3.57	3.53	3.81
O	3.04	3.33	4.05	3.60	3.69
F	*a*	2.59	4.45	3.83	4.17
Ne	3.71	3.54	3.95	3.91	4.65
Na	1.89	1.69	*a*	2.49	2.26
Mg	2.25	2.00	2.14	2.22	2.76
Al	2.30	2.31	2.29	*a*	2.45
Si	2.83	3.18	3.37	2.70	2.86
P	2.76	2.79	3.07	3.05	3.24
S	2.68	3.01	3.46	3.15	3.22
Cl	2.49	3.09	4.05	3.39	3.61
Ar	3.41	3.36	3.68	3.68	3.97

[a] Potential curves show points of inflection or up and down structures.

final parameter sets when they were clearly negligible. As shown in Table 3, ΔR_{rms} were found to be smaller than 0.16 Å. Oscillating terms in eq 4 were found to be negligible in many cases. Since fitting procedures were performed for an energy range between 0 and 1000 meV, fitted potential functions can thus be used in this energy range including thermal energies.

4. Discussion

4.1. Comparison of Outer Profiles of Molecules Predicted from the Total Electron Density and the Site−Site Potential.

When the repulsive interaction with a probe atom is mainly dominated by the overlap between wave functions, outer profiles of molecules are expected to be similar to the total electron density distributions. However, outer shapes of molecules probed by atoms are not so simple as those predicted from the electron distributions, as can be seen in Figures 4 and 5. Anisotropic interaction reduces the exchange repulsion energy effectively to deform outer profiles of molecules into various forms.

One simple way to construct intermolecular interaction potential functions is to utilize site−site potentials,[29] in which a molecule is regarded as being composed of a number of independent sites interacting with similar sites in neighboring molecules

$$V(R) = \sum_{i<j} V_{ij}(R_{ij}) \tag{5}$$

$$V_{ij}(R_{ij}) = A_{ij} \exp(-a_{ij}R_{ij}) - \frac{B_{ij}}{R_{ij}^{\,6}} \tag{6}$$

where A_{ij}, a_{ij}, and B_{ij} are characteristic parameters between sites i and j. Outer profiles of hydrogen molecule estimated from this potential using parameter values in refs 30 and 31 are drawn for some atomic probes in Figure 6(c). The *n*th lines from the outside correspond to the contours of $n \times 100$ meV. It is found

(29) Rigby, M.; Smith, E. B.; Wakeham, W. A.; Maitland, G. C. *The Forces between Molecules*; Clarendon: Oxford, 1986.
(30) Scott, R. A.; Scheraga, H. A. *J. Chem. Phys.* **1965**, *42*, 2209−2215.
(31) Abe, A.; Jernigan, R. L.; Flory, P. J. *J. Am. Chem. Soc.* **1966**, *88*, 631−639.

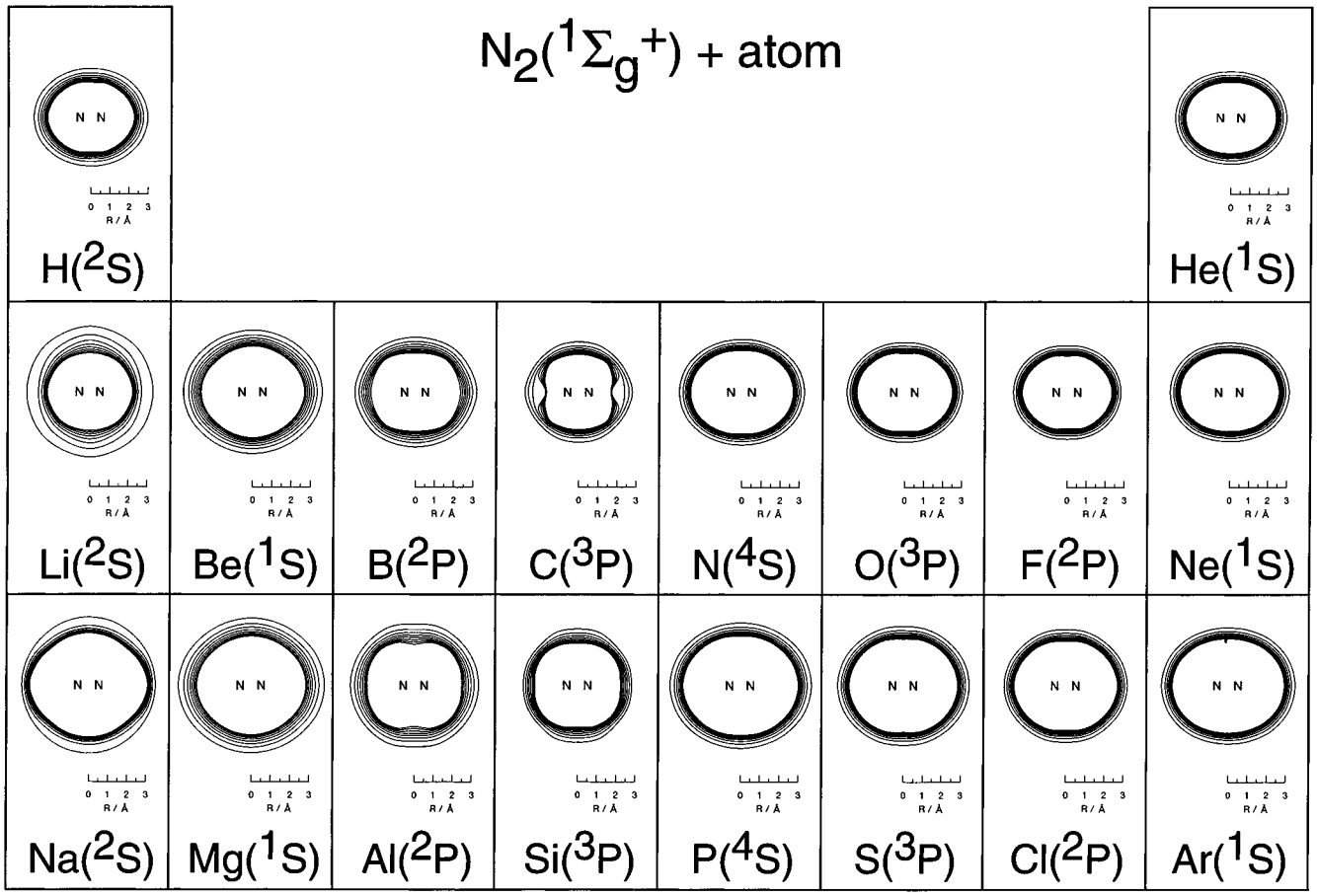

Figure 5. *Ab initio* isopotential energy contours of $N_2(^1\Sigma_g^+)$ in interaction with a probe atom from H(^{2}S) to Ar(^{1}S). The *n*th lines from the outside correspond to the contours of $n \times 100$ meV.

that outer profiles obtained with pair-potentials of exp-6 (Figure 6(c)) cannot adequately represent the variety of outer profiles of molecules (Figure 6(a)). Therefore, it is necessary to perform *ab initio* calculations in order to characterize the outer shape of molecules.

4.2. The Outer Profiles of Molecules Probed by Atoms. Obtained profiles in Figures 4 and 5 are considered to represent the intrinsic flexibility of molecular surfaces with the molecular skeletons being fixed. It should be noted that some of them are different from those expected by Lennard-Jones potentials usually used in molecular mechanics calculations[19,20] or those simply approximated by spheres of VDW radii widely employed in molecular modeling calculations.[6]

Figure 7 shows typical forms of the profiles for homonuclear diatomic molecules. The most typical form is the type 1 (prolate form) which is a prolate sphere with a long axis along the chemical bond. The type 2 (sphere form) is considered to be a deformed form of the standard prolate form by shrinkage along the bond axis. The type 3 (oblate form) appears by further shrinkage along the bond axis. The type 4 (dent form) can be produced when shrinkage occurs more locally along the bond axis. This form is double-dented like an apple. The type 5 (waist form) is, on the other hand, to be produced by circular shrinkage at right angles around the bond axis. Waist form looks like a shell of peanuts. The type 6 (lemon form) may appear by local shrinkage at oblique angles around the bond axis. Lemon form is like a spindle. The causes of the above various shapes being produced are individually discussed below.

4.2.1. Prolate Form. Prolate forms being longer for the molecular bond axis as the standard form of diatomic molecules are seen for H_2 with Li and Na (Figure 4) and N_2 with H, He,

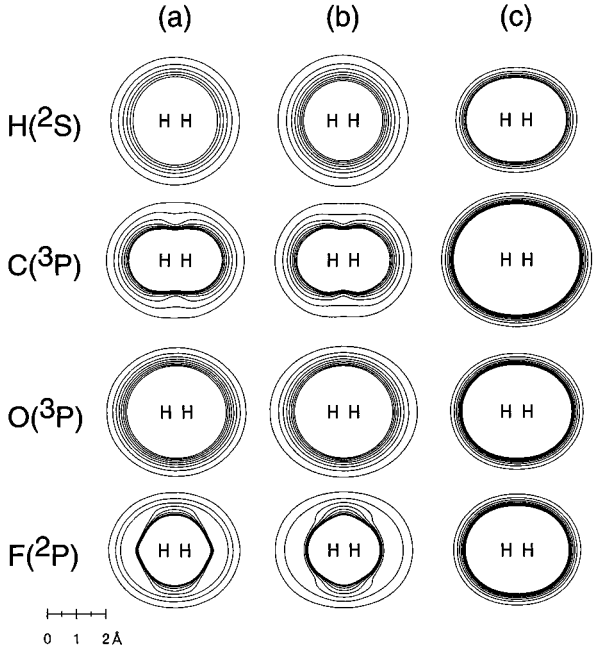

Figure 6. Isopotential energy contours for $H_2(^1\Sigma_g^+)$ + H(^{2}S), C(^{3}P), O(^{3}P), and F(^{2}P) by *ab initio* calculation (a), functional fitting (b), and site−site potentials (c). The *n*th lines from the outside correspond to the contours of $n \times 100$ meV.

N, O, F, Ne, P, S, Cl, and Ar (Figure 5). This tendency can also be seen in Figures 2 and 3, where potential energy curves for $\theta = 0°$ are mostly displaced to the longer distance with respect to those for $\theta = 90°$. The elongated shapes of molecules along the bond axis are a result of ordinary electron exchange

Table 3. Parameter Values (A_i, a_i, B_i, b_i, and c_i) and Root Mean Square Errors (ΔR_{rms})[a] Obtained from the Functional Fitting of Eqs 3 and 4 to the Potential Energy Surfaces of H_2 (a) and N_2 (b)[b]

	i	A_i/eV	a_i/Å^{-1}	B_i/eV	b_i/Å^{-2}	c_i/Å^{-1}	ΔR_{rms}/Å		i	A_i/eV	a_i/Å^{-1}	B_i/eV	b_i/Å^{-2}	c_i/Å^{-1}	ΔR_{rms}/Å
							(a) $H_2(^1\Sigma_g^+)$								
H	0	20.72	2.359	0.0				Ne	0	167.4	3.016	0.0			
	2	−1.985	193.5	0.0			0.0230		2	16.73	2.667	0.0			0.0462
He	0	207.6	3.520	0.0				Na	0	61.13	2.223	0.0			
	2	31.02	3.270	0.0			0.0055		2	18.33	2.188	0.0			0.1138
Li	0	25.50	2.025	0.0				Mg	0	97.60	2.191	0.0			
	2	10.27	2.042	0.0			0.1563		2	5.552	1.782	0.0			0.0371
Be	0	64.42	2.186	0.0				Al	0	81.17	2.442	0.0			
	2	7.615	2.553	0.0			0.0201		2	36.72	2.188	0.0			0.0272
B	0	91.52	2.746	15.52	1.478	0.7098		Si	0	126.3	2.987	0.0			
	2	2.613	1.446	−1.655	0.7529	0.6727	0.0184		2	41.59	2.334	0.0			0.0375
C	0	40.20	2.725	11.76	1.586	0.4821		P	0	109.8	2.249	0.0			
	2	31.62	2.815	−13.02	2.127	0.6564			2	2.985	2.249	0.0			0.0632
	4	−0.3080	54.05	−4.351	1.538	1.897	0.0178	S	0	118.7	2.479	0.0			
N	0	109.3	2.670	0.0					2	8.045	2.000	0.0			0.0419
	2	4.108	2.256	0.0			0.0486	Cl	0	101.6	2.656	0.0			
O	0	85.32	2.858	0.0					2	0.7928	1.047	0.0			0.0258
	2	1.868	1.471	0.0			0.0364	Ar	0	553.0	3.065	0.0			
F	0	25.66	2.589	76.55	2.387	0.4566			2	9.861	2.106	0.0			0.0301
	2	12.68	2.332	53.07	1.804	0.4580									
	4	−0.6377	23.30	19.87	2.812	0.0003	0.0264								
							(b) $N_2(^1\Sigma_g^+)$								
H	0	135.4	2.577	0.0				Ne	0	117.9	2.219	0.0			
	2	63.43	2.296	0.0			0.0491		2	93.13	2.203	0.0			0.1258
He	0	114.2	2.420	0.0				Na	0	4344.8	2.723	41.92	0.4271	0.3156	
	2	93.00	2.394	0.0			0.1020		2	1057.6	10.92	117.4	0.4418	0.1437	
Li	0	560.4	2.641	−16.17	0.4109	0.1593			4	196.4	1.710	38.89	0.3160	0.2033	0.0007
	2	189.3	2.875	33.93	0.6406	0.2425		Mg	0	1184.7	2.969	−1.853	0.2395	0.3303	
	4	10.69	1.903	7.539	0.5740	0.2548	0.0019		2	500.7	2.502	7.013	0.4140	0.4067	
Be	0	1425.4	3.353	−12.42	0.4489	0.2747			4	175.9	2.685	0.1014	4.392	0.1006	0.0364
	2	448.7	2.941	−14.12	0.4272	0.1958		Al	0	858.6	3.375	7.229	0.4083	0.0011	
	4	122.6	10.49	0.7419	0.2920	0.0031	0.0002		2	342.4	2.790	17.07	1.220	0.0223	
B	0	621.4	2.849	572.1	1.346	0.2662			4	−158.3	14.27	−55.54	0.7821	0.1029	0.0001
	2	18.53	1.785	0.9721	5.672	0.1234		Si	0	837.6	3.023	752.2	1.831	0.0000	
	4	−94.37	22.24	61.81	0.8843	0.5913	0.0532		2	75.71	155.6	115.0	0.9131	0.1876	
C	0	887.7	3.339	1156.9	1.744	0.2662			4	−99.02	1.982	−54.69	0.5814	0.2554	0.0013
	2	−23.67	5965.	1110.7	1.977	0.2561		P	0	1007.8	2.596	0.0			
	4	−110.3	3.540	122.9	1.162	0.6516	0.0508		2	994.9	2.688	0.0			0.0534
N	0	105.8	2.067	0.0				S	0	1017.3	2.731	0.0			
	2	99.02	2.181	0.0			0.1333		2	994.5	2.796	0.0			0.0542
O	0	105.7	2.209	0.0				Cl	0	1009.4	2.881	0.0			
	2	99.28	2.289	0.0			0.1227		2	996.3	2.977	0.0			0.0612
F	0	130.5	2.460	0.0				Ar	0	1000.0	2.693	0.0			
	2	92.48	2.441	0.0			0.1059		2	1000.0	2.737	0.0			0.0746

[a] Obtained from the data in the energy region of 100−800 meV. [b] For each atom, the values of zero ($i = 0$) and second order ($i = 2$) are listed. The values of fourth order ($i = 4$) are also listed when they are not negligible.

interactions, which can be compared with the total electron density distributions of molecules.

4.2.2. Sphere Form. Sphere forms are found for H_2 probed by H, He, Be, N, Ne, Mg, P, and Ar (Figure 4). Correspondingly, potential energy curves for $\theta = 0°$, 45°, and 90° in Figure 2 are nearly identical. Sphere form can also appear when shrinkage occurs along perpendicular directions for an oblate form; an example can be seen for N_2 with Li at ca. 480 meV (Figure 5). The cause of the round profiles of H_2 is the smaller repulsive interaction for $\theta = 0°$ than those for $\theta = 90°$, because the antibonding molecular orbital of H_2 can reduce the repulsive interaction energy between H_2 and a probe atom when the geometry is collinear ($\theta = 0°$).

4.2.3. Oblate Form. An oblate form is found for N_2 with Li at ca. 100−400 meV (Figure 5). The potential energy curve for $\theta = 0°$ has a point of inflection and is considerably deformed from the exponential form with respect to that for $\theta = 90°$ (Figure 3). These unusual forms for N_2 with Li are due to peculiar interactions of 2s and 2p orbitals in the probe atom with occupied orbitals in the molecule.

An analysis of difference in electron densities between the interacting and isolated systems provides a clear vision. Figure 8(a) shows the difference electron density contour map ($\Delta\rho$ map) for N_2 + Li in a collinear geometry at $R = 3.0$ Å. Dotted lines indicate that $\Delta\rho$ is negative (electron densities for interacting systems decrease in comparison with those for summations of electron densities for isolated systems). Contours of $\Delta\rho = 0$ are drawn by dashed lines. The nth lines from the 0-lines correspond to $|\Delta\rho| = 2^{n-1} \times 5.0 \times 10^{-5}$ au^{-3}. Electron densities between N_2 and Li decreases, which brings repulsive forces between them. It is of note that the electron densities are considerably increased in the outward regions around the Li atom. This is clearly due to conversion of the 2s electron into an sp hybrid.

The 2s−2p hybridization for N_2 + Li is highly anisotropic, and the extent of 2p mixing for collinear direction ($\theta = 0°$) is considerably larger than those for vertical direction ($\theta = 90°$).[32] The sp hybridization effect common in alkali and alkaline earth metal atoms is the most remarkable for Li due to the smallest ns-np ($n \geq 2$) energy separations; the separation becomes larger for alkaline earth metal atoms (2.70−2.73 eV) than for alkali metal atoms (1.84−2.11 eV).

(32) Ohno, K.; Takami, T.; Mitsuke, K.; Ishida, T. *J. Chem. Phys.* **1991**, *94*, 2675−2687.

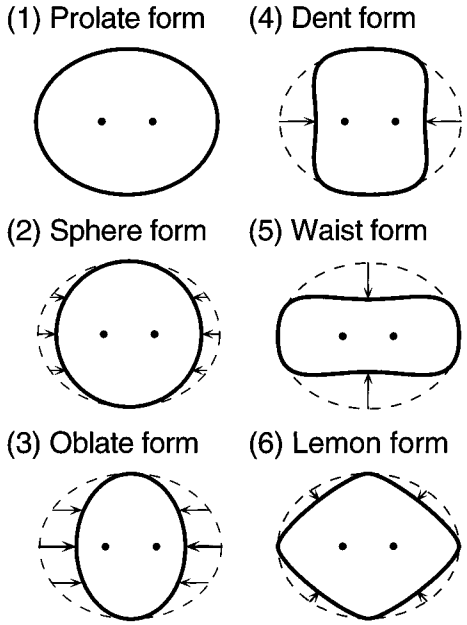

Figure 7. Prototypes of the profiles for homonuclear diatomic molecules. (1) Prolate form, (2) sphere form, (3) oblate form, (4) dent form, (5) waist form, and (6) lemon form. Arrows indicate anisotropic interactions reducing exchange repulsions.

4.2.4. Dent Form. A typical example of dent form is found for N_2 with C at higher energies larger than 400 meV (Figure 5). Potential energy curves of $\theta = 0°$ for $N_2 + C$ and $N_2 + B$ in Figure 3 show minima at short distances of $R = 1.84$ and 2.05 Å, respectively. The appearance of this form is attributed to a strong donative interaction of σ_{HOMO} in the molecule with a probe 2p orbital in the collinear direction.

As shown in Figure 8(b), the $\Delta\rho$ map for the potential minimum reveals a considerable σ electron donation from the HOMO of σ-type (σ_{HOMO}) in N_2 to the vacant $2p_z$ orbital on C atom and a small amount of π back-donation from $2p_x$ and $2p_y$ orbitals to the π_{LUMO} in N_2. This overwhelming importance of the σ donation over the π back-donation is consistent with the absence of respective potential minima for $N_2 + Al$ ($\theta = 0°$) and $N_2 + Si$ ($\theta = 0°$) in Figure 3, since the 3p levels of Al and Si are much higher than the 2p level of B to result in the much smaller σ donation.

While in the collinear interaction with H_2 molecule, np_x and np_y ($n \geq 2$) orbitals on probe atoms cannot interact with σ_{HOMO} and σ_{LUMO} in H_2. Since the back-donative contribution of σ_{LUMO} reduces the electron donation to np_z ($n \geq 2$) orbital, potential energy curves of $\theta = 0°$ for H_2 with Group 13 and Group 14 atoms are very similar, without minima at short distances in Figure 2.

4.2.5. Waist Form. An example of waist form is found for H_2 with C at higher energies larger than 300 meV (Figure 4). Unusual behavior in the profiles is more clearly seen in Figure 2; the curve for $\theta = 90°$ has a point of inflection at $R \approx 1.5$ Å. An inadequately deformed form toward waist form can be seen for H_2 with B at higher energies (Figure 4). For H_2 with Al and Si (Figure 4), prolate forms toward waist forms are considered to be seen. The interaction leading to waist form is also attributed to a strong donative interaction of σ_{HOMO} in the molecule with a probe 2p orbital in the perpendicular direction. The $\Delta\rho$ map for $R = 1.5$ Å reveals a considerable σ electron donation from the σ_{HOMO} in H_2 to the vacant C $2p_z$ orbital in Figure 8(c). The importance of the donation effect of the σ_{HOMO} is consistent with the absence of respective unusual structures for $H_2 + Al$ ($\theta = 90°$) and $H_2 + Si$ ($\theta = 90°$) in Figure 3.

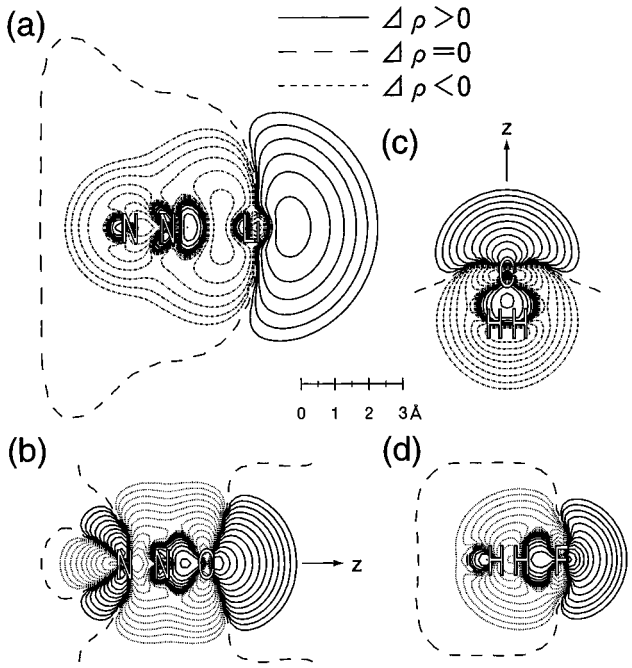

Figure 8. Difference electron density contour maps. Contours of $\Delta\rho = 0$ are drawn with dashed lines. The nth dotted ($\Delta\rho < 0$) or solid lines ($\Delta\rho > 0$) from the 0-lines correspond to $|\Delta\rho| = 2^{n-1} \times 5.0 \times 10^{-5}$ au.$^{-3}$ (a) $N_2(^1\Sigma_g^+) + Li(^2S)$ for $\theta = 0°$ at $R = 3.0$ Å. (b) $N_2(^1\Sigma_g^+) + C(^3P)$ for $\theta = 0°$ at $R = 1.84$ Å. (c) $H_2(^1\Sigma_g^+) + C(^3P)$ for $\theta = 90°$ at $R = 1.5$ Å. (d) $H_2(^1\Sigma_g^+) + F(^2P)$ for $\theta = 0°$ at $R = 1.53$ Å.

4.2.6. Lemon Form. Some examples to be assigned as lemon forms are found for N_2 with Na, Be, and Mg (Figure 5). Separations of corresponding potential energy curves between $\theta = 45°$ and 90° are considerably narrowed (Figure 3). In these cases, a back-donative interaction of the probe ns ($n \geq 2$) orbital with π_{LUMO} in the molecule effectively occurs at oblique angles, because the π_{LUMO} has nodal planes at $\theta = 0°$ and 90°. The specific effect of the π_{LUMO} around $\theta = 45°$ is remarkable for the low *IP* probes of alkali and alkaline earth metal atoms, although for Li atom the 2s−2p hybridization is dominant.

4.2.7. Other Characteristic Profiles. In the case of N_2 with Al, attractive interactions reducing the exchange repulsion energy are involved at both $\theta = 0°$ and 90°, which can be related with both the dent form and the waist form. In this case, the back-donation to the π_{LUMO} rather than σ electron donation is superior due to the much higher 3p level than the 2p level of B. This is responsible for the appearance of the deformed structure for $N_2 + Al$ ($\theta = 90°$).

In the case of $H_2 + F$ ($\theta = 0°$), a short-range potential well is found at $R = 1.53$ Å. This unusual structure can be compared with those for $N_2 + C$ ($\theta = 0°$) in Figure 3 and $H_2 + C$ ($\theta = 90°$) in Figure 2, in which electron donation from the molecule to the probe atom is remarkable (Figure 8 (parts b and c)). The $\Delta\rho$ map for $H_2 + F$ ($\theta = 0°$) at $R = 1.53$ Å in Figure 8(d) shows also marked electron donation from the σ_{HOMO} orbital to the singly occupied $2p_z$ orbital. The preference of the perpendicular geometry (the T-shaped structure) in the short-range interactions for $H_2 + B$ and $H_2 + C$ can be attributed to the presence of the bonding electron in the b_2 orbital including an inplane p orbital in contrast to the electron configuration for the collinear geometry. On the other hand, for $H_2 + F$, the 2p level of the F atom becomes very deep to make the bonding contribution of the b_2 orbital ineffective due to the increased energy gap between σ_{LUMO} and 2p levels. Therefore, the ionic interactions including inductive effects are considered to become

more effective in connection with the more polarizable geometry.

4.3. Flexibility of Molecules. Mechanical deformation of molecules has been studied by molecular mechanics calculations.[19,20] Flexibility of molecules in interacting with other systems can be classified into two types: one is related to the internal deformation of molecular skeletons and the other is related to the nature of molecular surfaces. In molecular mechanics calculations,[19,20] the former type flexibility of molecules is taken into account by internal force fields related to molecular vibrations, while the latter type flexibility of molecules is approximated by pair-potentials such as Lennard-Jones potentials. In order to elucidate the latter type flexibility (nonreactive flexibility) of molecules, molecular geometries were fixed at the ground-state structures in the present study.

5. Conclusion

Surface characteristics of hydrogen and nitrogen molecules have been systematically studied using a series of ground-state atoms from H to Ar as a probe.

(1) Periodicity and some interesting patterns have been found for outer profiles of molecules. This is a consequence of electronic configurations of atomic probes. Energy levels and spatial distribution of orbitals are key factors governing the profiles.

(2) When the exchange repulsion energy due to antibonding electrons is dominant, repulsive walls of potential energy curves show a simple exponential decay with hardness depending on the ionization potentials. This means that repulsive parts of potential functions are not the Lennard-Jones type but the pure exponential type.

(3) When anisotropic interactions reduce the exchange repulsion energy effectively, outer shapes of molecules probed by atoms are deformed into various forms. Even for homonuclear diatomic molecules such as hydrogen and nitrogen, several types of interesting shapes have been found: pure sphere form being produced by shrinkage along the long axis of the prolate form, oblate form being longer in the perpendicular direction with respect to the chemical bond, axially dented form like an apple, waist form like a shell of peanuts, and lemon form shrunk at oblique angles.

Acknowledgment. This work has been partly supported by a Grant in Aid for Scientific Research from the Japanese Ministry of Education, Science, and Culture and also partly supported by a Grant in Aid from Toyota Physical and Chemical Research Institute. The authors wish to thank Dr. Hideo Yamakado for helpful comments and discussion.

JA963376E